RSC Advances

ROYAL SOCIETY OF CHEMISTRY

www.rsc.org/advances

Table of contents

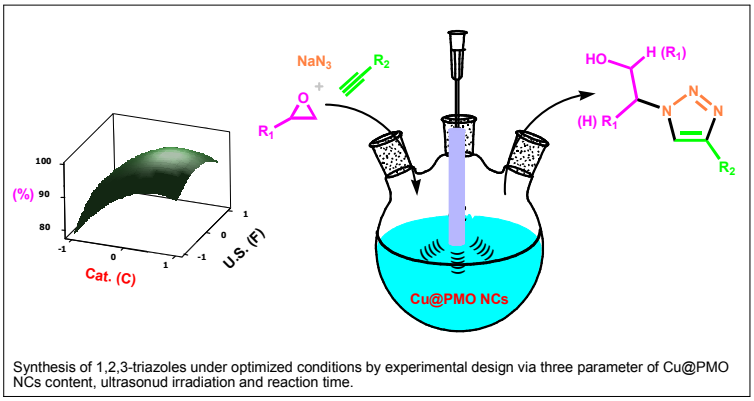

Synthesis of 1,2,3-triazoles under optimized conditions by experimental design via three parameter of Cu@PMO NCs content, ultrasonud irradiation and reaction time.

RSC Advances

RSC Publishing

ARTICLE

Highly efficient copper-imprinted functionalized mesoporous organosilica nanocomposites as a new recyclable catalyst for click synthesis of 1,2,3-triazole derivatives under ultrasound irradiation: Multivariate study by factorial design of experiments

Cite this: DOI: 10.1039/x0xx00000x

Hossein Naeimi*[1], Vajihe Nejadshafiee[1] and Saeed Masoum[2]

A green and convenient study to one-pot synthesis of β-hydroxy-1,2,3-triazoles through a three component coupling a variety of epoxides and alkynes over copper-imprinted periodic mesoporous organosilica nanocomposites (Cu@PMO NCs) under ultrasound irradiation in the present of water as solvent, has been developed. An experimental design [Box-Behnken design (BBD)] adopting surface response could efficiently be applied for the modeling of catalytic synthesis of β-hydroxy-1,2,3-triazole, and it is an economical way of obtaining the optimal reaction conditions based on restrict number of experiments. Reactions were performed in ultrasound equipment and different variables such as catalyst amount, ultrasound irradiation frequency and ultrasound time were investigated. The use of water as natural solvent for biological chemistry, the mathematic model proposal for satisfactorily representation of the process and good correlation among the experimental results and the theoretical values predicted by model equation, ultrasound irradiation, reusability of the catalyst up to six runs without appreciable loss of activity, short reaction times and high yields of products make this procedure greener than the other works.

Received ooth
Accepted ooth

DOI: 10.1039/x0xx00000x

www.rsc.org/

Introduction

According to the principle of green chemistry, synthetic methods should be designed to use substances and reaction condition that exhibit little or no toxicity to human health and environment. Thus, recent achievements in chemical efficiency have focused on application of heterogeneous catalysts in the organic reactions. The majority of novel heterogeneous catalysts are based on silica supports, primarily because silica displays some advantageous properties, such as excellent chemical and thermal stability, porosity, good accessibility and the fact that organic groups can be robustly imprinted to the periodic mesoporous organosilica (PMO) or anchored to the silica framework to provide catalytic centers[1,2]. A wide range of studies have been carried out on the preparation of molecular-imprinting silica hybrids based on inorganic mediums, such as surface immobilization on periodic mesoporous silica materials (SBA-15, MCM-41) and silica particles[3–6]. Molecular imprinting on the PMO is considered an important technique for preparing materials with selective recognition properties owing to its cost effectiveness and ease of use compared to complicated biological systems[7–9].

[1]Department of Organic Chemistry, Faculty of Chemistry, University of Kashan, Kashan, 87317, I.R. Iran; Tel: 983615912388; Fax; 983615912397; Email: naeimi@kashanu.ac.ir.
[2]Department of Analytical Chemistry, Faculty of Chemistry, University of Kashan, Kashan, 87317, I.R. Iran.

Generally, an interesting feature of metal-imprinted PMO hybrid is its convenient modification with a relatively high degree of functionality and ordered mesostructures modification that provides a wide range of applications including heterogeneous catalyst, selective recognition, separation and sensor devices[10,11]. The formation of 1,2,3-triazoles derivatives was proceeded through the copper-catalyzed Huisgen 1,3-dipolar cycloaddition of azides and alkynes using CuAAC as catalyst[12–14]. Recently, this reaction under different heterogeneous catalysts with source of copper in water was developped[15–22]. One-pot synthesis of β-hydroxy-1,2,3-triazoles from epoxides, linked to the dipolar cycloaddition with azide and alkynes has been reported through some heterogeneous catalytic system such as; copper nanocomposites on activated carbon[23,24], copper (I)-modified zeolites[25], copper(I)@phosphorated SiO_2[26], porphyrinato copper nanocomposites[27], Cu[N_2,N_6-bis(2-hydroxyphenyl) pyridine-2,6-dicarbox-amidate][28]. Ultrasound techniques have increasingly been used in organic synthesis during the last few years. Compared with traditional methods, this method can give higher yields in shorter reaction times and under milder conditions[29]. Ultrasound irradiation has some potential effects on a heterogeneous catalytic system, like increase of active catalyst surface area, promotion of cavitation bubble formation and removal of impurities deposited on the catalyst [30]. Moreover, click synthesis of 1,2,3-triazole derivatives from a variety of alkyl halides or organoic azides and alkynes under

ultrasound irradiation usage green catalysts such as copper and iron are attractive in the growing field of green and more sustainable chemistry [31,32].

In continuation of our work on the preparation and reactivity of hybrid copper-imprinted periodic mesoporous organosilica (Cu@PMO NCs), it was found that is a very suitable catalyst for synthesis of *β*-hydroxy-1,2,3-triazoles under thermal conditions. Herein, we hope to report a green and convenient approach to three-component synthesis of *β*-hydroxy-1,2,3-triazoles from epoxides, terminal alkynes and sodium azide catalyzed by Cu@PMO NCs under ultrasound irradiation in water at room temperature. To find out the suitable condition for the reaction, the experimental design [Box-Behnken design (BBD)][33,34] using surface response was performed, and hence three variants of catalyst amount, ultrasound irradiation frequency and ultrasound time were selected. This investigation can be assessed the optimized conditions so that the best results in terms of organic reaction including products yield, reaction times and stability and recyclability of catalyst.

Experimental

Experimental design

A Box-Behnken design (BBD) composed of three variables, ranging over three levels was used to maximize the response of Cu@PMO NCs activities in terms of *β*-hydroxy-1,2,3-triazole yields and hence reduce the requirement for a higher number of experiments without compromising the results. The BBD 15 (2^k+2^k+1, k=3) was applied with central points triplicate for the reaction. The three variables and their levels are described below. Variables were chosen in order to add economic value by reducing the process cost. The proposal includes parameters such as lower catalyst load and ultrasound time. Ultrasound irradiation was chosen considering the high *β*-hydroxy-1,2,3-triazole production at room temperature. The experiments design and results for the reaction over Cu@PMO NCs were listed in Table 1.

Table 1 Experimental design and results of BBD for *β*-hydroxy-1,2,3-triazole (**3a**).

Entry	Cu@PMO NCs content (%)[a]	Ultrasound irradiation frequency (kHz)	Ultrasound time	Yield (%)
1	0.005 (0)	40 (0)	7 (0)	98
2	0.01 (+)	40 (0)	10 (+)	95
3	0.003 (-)	40 (0)	5 (-)	80
4	0.005 (0)	30 (-)	5 (-)	84
5	0.01 (+)	30 (-)	7 (0)	92
6	0.005 (0)	40 (0)	7 (0)	98
7	0.003 (-)	40 (0)	10 (+)	80
8	0.005 (0)	40 (0)	7 (0)	98
9	0.01 (+)	40 (0)	5 (-)	95
10	0.005 (0)	30 (-)	10 (+)	93
11	0.005 (0)	50 (+)	5 (-)	93
12	0.005 (0)	50 (+)	10 (+)	85
13	0.01 (+)	50 (+)	7 (0)	90
14	0.003 (-)	50 (+)	7 (0)	84
15	0.003 (-)	30 (-)	7 (0)	80

[a] (+ upper, 0 central, - lower).

General information

All chemicals solvents were purchased from commercial suppliers. FT-IR spectra were obtained as KBr pellets on a Perkin-Elmer 781 spectrophotometer and on an impact 400 Nicolet FT-IR spectrophotometer. The XRD patterns were recorded on an X-ray diffractometer (Bruker, D8 ADVANCE, Germany) using a Cu-Ka radiation (λ = 0.154056 nm) in the range 2θ=0.5–5°. Thermogravimetric analysis (TGA) was carried out on STA 503 WinTA instrument at a heating rate of 10 ºC min^{-1} under nitrogen (N_2) atmosphere. The N_2 adsorption/desorption analysis (BET) was performed at -196 °C using an automated gas adsorption analyzer (Tristar 3000, Micromeritics). The surface morphology of the supported catalyst was studied by scanning electron microscopy. FE-SEM and elemental analysis were carried out using a Jeol SEM instrument (model- VEGA/TESCAN) combined with an INCA instrument for energy dispersive X-ray spectroscopy scanning electron microscopy (EDS-SEM), with scanning electron electrode at 15 kV. The diffuse reflectance UV-visible of samples was recorded at room temperature on Perkin-Elmer 35 LAMDA instrument using barium sulfate as a reference. Liquid NMR was obtained on a Bruker DRX-400 MHz Bruker Avance instrument using $CDCl_3$ and DMSO as solvent and TMS as an internal standard. The Bandelin ultrasonic HD 3200 with probe model KE 76, 6 mm diameter, was used to produce ultrasonic irradiation and homogenizing the reaction mixture.

Preparation of organometallic-LCu

1,1-[2,4,6-Triyl-1,3,5-triazinebis(nitrilomethylidine)]bis-(phenol) -ligand (**1**) was synthesized by dissolving salicylaldehyde (0.214 g, 2 mmol) and melamine (0.126 g, 1.0 mmol) in 5 mL of methanol and three drops of acetic acid. The reaction mixture was heated under

reflux at 100 ºC for 4 h. After the completion of the reaction, ligand product was filtered, washed with water, dried at ambient temperature and resulting in the formation of orange solid in 98 % yield. IR (KBr): ν= 3468, 3416, 3332, 3129, 1654, 1552, 1439, 1272. ^{1}H NMR (400 MHz, DMSO) δ= 10.71 (s, 1 H, O-H), 10.24 (s, 1H, O-H), 7.65-6.63 (m, 8 H, aromatic), 6.04 (s, 2H, N-H).). ^{13}C NMR (100 MHz, DMSO) δ= 178.34, 174.44, 167.81, 164.94, 130.40, 128.82, 125.61, 121.09, 119.94. Anal. calcd for C, H, N: 61.07 (C), 4.22 (H), 25.14 (N); found: 61.10 (C), 4.18 (H), 25.15 (N).

To prepare the organometallic (**2**) (LCu), the ligand (0. 332 g, 1 mmol) was dissolved in 15 mL of dimethylformamide and treated with copper acetate monohydrate ($Cu(OAc)_2$. H_2O), heated under reflux for 3 h. Finally, the formed metal–ligand complex was filtered, washed with 96 % ethanol (100 mL) and dried for 1 day under vacuum to produce complex as brown crystals in 95 % yield. IR (KBr): ν= 3466, 3419, 3343, 3131, 1650, 1548, 1438, 1204.

Preparation of copper-imprinted organopolysilane precursor

The copper-imprinted organopolysilane precursor (**3**) was obtained as follows; 0.5 g (1.3 mmol) of LCu (**2**) was dissolved in 60 mL of dry ethanol. To this, 0.5 mL (2.6 mmol) of 3-chloropropytrimethoxysilane was added drop wise under a N_2 atmosphere in the presence of NaH as base. The reaction mixture was stirred at 60 ºC for 24 h under nitrogen atmosphere. Subsequently, the reaction mixture was filtered, concentrated under vacuum, purified with diethylether (3 × 50 mL) and dried under vacuum and copper-imprinted organopolysilane precursor (3) was obtained in 90 % yield. IR (KBr): ν= 3402, 2922, 2852, 1558, 1460, 1266. Anal. Calcd for C, H, N: 48.35 (C), 5.60 (H), 11.67 (N). Found: 47.29 (C), 5.62 (H), 10.82 (N).

Synthesis of copper-imprinted periodic mesoporous organosilica nanocomposite (Cu@PMO NCs)

Copper-imprinted periodic mesoporous organosilica nanocomposite (Cu@PMO NCs) was prepared by tri constituent, copper-imprinted organopolysilane precursor, oligomer silicates from tetraethylorthosilicate (TEOS), and cetyltrimethyl ammonium bromide (CTAB) template. In a typical preparation, 1.0 g of CTAB (2.74 mmol) was dissolved in 47 mL of distilled water. The solution was stirred for 10 min, followed by the addition of 11 mL ammonia (25 %) and stirred for a further 30 min to obtain a clear solution. A premixed propanol solution of organopolysilane precursor (**3**) and TEOS were added to the surfactant solution. The molar composition of the final synthetic mixture was TEOS: ion-imprinted organopolysilane precursor (**3**): CTAB: NH_3: H_2O: propanol = (1 + x): x: 0.12: 8.0: 114: 7; where, x = 0.05 for Cu@PMO NCs, respectively. The reaction mixture was stirred at 35 ºC for 24 h. The final mixture was then crystallized at 90 ºC for 24 h. The resulting solid was filtered and washed with deionized water, and dried in a vacuum at 60 ºC for 12 h. The surfactant was removed by extracting the solid with a 0.05 M ethanolic HCl solution at 60 ºC for 6 h (50 mL of 0.05 ethanolic HCl for 1 g of solid material). The obtained material was designated as Cu@PMO NCs.

Ultrasound-promoted typical procedure for synthesis of *β*-hydroxy-1,2,3-triazoles (3a)

A 25 mL Erlenmeyer flask was charged with the styrene oxide (1 mmol), NaN_3 (72 mg, 1.1 mmol), the alkyne (1 mmol), Cu@PMO NCs (7 mg, 0.33 mol %) in H_2O (3 mL). The reaction flask was located in the ultrasounic probe and irradiation under 40 kHz at room temperature for 7 min. The solid product was collected from the reaction mixture. In order to separate the catalyst, the product was dissolved in hot methanol, subsequently, the whole mixture was directly passed through a sintered glass filter funnel, and the solvent was removed in vacuum to give the corresponding product **3a** in 99 % yield and also other derivatives of *β*-hydroxy-1,2,3-triazole (3b-l) were synthesized with this procedure.

2-Phenyl-2-(4-phenyl-1H-1,2,3-triazol-1-yl)ethanol (3a)
Pale yellow solid: mp. 125-127 ^{o}C, Lit[23] (mp. 125.5-127 ^{o}C). IR (KBr): ν= 693, 758, 1045, 1079, 1242, 1436, 1463, 1493, 1595, 2928, 3064, 3087, 3140, 3346. ^{1}H NMR(400 MHz, $CDCl_3$) δ= 7.81-7.79 (m, 3H), 7.70 (s, 1H), 7.43-7.39 (m, 6 H) 7.34 (s, 1H), 5.68 (dd, ^{3}J(H,H)= 8 Hz, ^{3}J=3.9 Hz, 1H), 4.68-4.61 (dd, ^{3}J(H-H)= 12.4 Hz, ^{3}J(H-H)= 7.6 Hz, 1H), 4.26-4.21 (dd, ^{3}J(H-H)= 14.4 Hz, ^{3}J(H-H)= 3.6 Hz, 1H), 3.22 (t, ^{3}J(H, H) = 6.8 Hz; 1H, OH).

***2*-(4-Phenyl-1H-1,2,3-triazol-1-yl)-1-p-tolylethanol (3b)**
Yellow solid: mp. 125 ^{o}C-127 ^{o}C, Lit [35] (mp. 124-126 ^{o}C). IR (KBr): ν= 696, 724, 755, 1047, 1075, 1008, 1185, 1220, 1380, 1457, 1496, 2927, 3029, 3092, 3418. ^{1}H NMR(400 MHz, $CDCl_3$) δ= 7.69-7.66 (m, 3H), 7.39 (m, 3H), 7.27-7.21 (m, 3H) , 5.68-5.66 (dd, ^{3}J(H,H)= 8 Hz, ^{3}J=3.2 Hz, 1H), 4.66-4.61 (dd, ^{3}J(H-H)= 12.6 Hz, ^{3}J(H-H)= 8.4Hz, 1H), 4.24-4.20 (dd, ^{3}J(H-H)= 9 Hz, ^{3}J(H-H)= 3.6 Hz, 1H), 2.38(s, 3H), 2.36 (t, ^{3}J(H, H) = 2.8 Hz; 1H, OH).

2-(4-Phenyl-1H-1,2,3-triazol-1-yl) cyclohexanol (3c)
Yellow solid: mp. 168-171 ^{o}C, Lit[23] (mp. 168-171 ^{o}C). IR (KBr): ν= 699, 768, 713, 1053, 1083, 1234, 1441, 2858, 2937, 3119, 3307. ^{1}H NMR (400 MHz, $CDCl_3$) δ= 7.79 (s, 1H), 7.74-7.72 (m, 2H), 7.40-7.37 (m, 2H) 7.33-7.30 (s, 1H), 4.19-4.09 (m, 3H), 4.01-1.90 (m, 4H), 2.25-2.22 (m, 2H), 1.51-1.26 (m, 2H).

1-(4-Phenyl-1H-1,2,3-triazol)hexan-2-ol (3d)
Cream solid: mp. 92-94 ^{o}C, Lit[35] (mp. 91-93 ^{o}C). IR (KBr): ν= 694, 764, 1087, 1138, 1227, 1463, 2862, 2925, 2959, 3141, 3248, 3408. ^{1}H NMR(400 MHz, $CDCl_3$) δ= 7.85 (s, 1H), 7.77-7.75 (m, 2H), 7.42-7.40 (m, 2H), 7.34-7.32 (m, 1H) , 4.52-4.49 (m, 2H), 4.29-4.24 (m, 1H), 4.15-4.13 (m, 1H), 1.57-1.51 (m, 3H), 1.44-1.37 (m, 3H), 0.95-0.92 (t, 3H). ^{13}C NMR (100 MHz, $CDCl_3$) δ= 147.27, 130.33, 128.78, 128.06, 125.53, 121.16, 70.44, 56.34, 34.17, 30.77, 28.01, 22.59, 13.99.

1-(4-Phenyl-1H-1,2,3-triazol-1-yl)butan-2-ol (3e)
White solid: mp. 110-111 ^{o}C, Lit[26] (mp. 110-111 ^{o}C). IR (KBr): ν= 694, 763, 982, 1078, 1136, 1228, 1457, 1617, 2926, 2962, 3139, 3254, 3419. ^{1}H NMR (400 MHz, $CDCl_3$) δ= 7.87 (s, 1H), 7.81-7.79 (m, 2H), 7.44-7.40 (m, 2H), 7.34 (m, 1H), 4.55-4.51 (dd, ^{3}J(H-H)= 14 Hz, 1H), 4.33-4.29 (dd, ^{3}J(H-H)= 13.8 Hz, ^{2}J(H-H)= 7.6 Hz, 1H), 2.66-2.65 (d, ^{3}J(H-H)= 4.4 Hz, 1H), 1.66-1.53 (m, 2H), 1.09-1.05 (t, 3H). ^{13}C NMR (100 MHz, $CDCl_3$) δ= 147.44, 130.40, 128.82, 128.12, 125.61, 121.09, 71.86, 55.84, 27.48, 9.81.

1-Phenoxy-3-(4-phenyl-1H-1,2,3-triazol-1-yl)propan-2-ol (3f)
Pale yellow solid: mp. 125-127 ^{o}C, Lit[27] (mp. 125.5-126 ^{o}C). IR (KBr): ν= 691, 755, 982, 1043, 1245, 1494, 1595, 2867, 2927, 3087,

3429. ^{1}H NMR(400 MHz, $CDCl_3$) δ= 7.89 (s, 1H), 7.75-7.73 (m, 2H), 7.41-7.38 (m, 2H), 7.32-7.27 (m, 3H) , 7.02-6.93 (m, 1H), 6.93-6.91 (m, 2H), 4.75-4.73 (m, 1H), 4.56-4.54 (m, 2H), 4.23-4.04 (m, 2H), 3.95-3.76 (m, 1H).

3-Isoproxy-2-(4-phenyl-1H-1,2,3-triazol-1-yl)propan-1-ol (3g)
Yellow solid: mp. 61-63 °C, Lit[26] (mp. 61-63 °C). R (KBr): ν= 695, 765, 924, 975, 1078, 1127, 1228, 1373, 1468, 2866, 2973, 3062, 3138, 3425. ^{1}H NMR(400 MHz, $CDCl_3$) δ= 7.91 (s, 1H), 7.79-7.77 (m, 2H), 7.42-7.38 (m, 2H), 7.34-7.30 (m, 1H) , 4.61-4.57 (dd, ^{3}J(H-H)= 12 Hz, ^{2}J(H-H)= 2.8 Hz, 1H), 4.64-4.41 (dd, ^{3}J(H-H)= 14 Hz, ^{2}J(H-H)= 4 Hz, 1H), 4.22 (m, 1H), 3.64-3.58 (m, 1H), 3.53-3.50 (dd, ^{3}J(H-H)= 8 Hz, ^{3}J(H-H)= 4.4 Hz, 1H), 3.40-3.36 (dd, ^{3}J(H-H)= 10 Hz, ^{3}J(H-H)= 4 Hz, 1H), 1.16-1.17 (t, 6H). ^{13}C NMR (100 MHz, $CDCl_3$) δ= 131.55, 130.36, 129.94, 129.21, 126.72, 122.49, 73.59, 70.45, 70.18, 54.49, 23.14.

2-Hydroxy-3-(4-phenyl-1H-1,2,3-triazol-1-yl)propyl acrylate (3h)
Livid solid: mp. 101-103 °C, Lit[26] (mp. 101-103 °C). IR (KBr): ν= 692, 756, 1044, 1246, 1494, 1596, 2925, 3087, 3425. ^{1}H NMR(400 MHz, $CDCl_3$) δ= 7.91 (s, 1H), 7.79-7.77 (m, 1H), 7.43-7.40 (m, 2H), 7.35-7.31 (m, 2H) , 7.02-6.99 (t, 1H), 6.93-6.91 (m, 2H), 4.22 (m, 1H), 3.64-3.58 (m, 1H), 4.07-3.98 (m, 1H), 3.38-3.37 (m, 1H). ^{13}C NMR (100 MHz, $CDCl_3$) δ= 158.25, 147.29, 130.10, 129.63, 128.86, 128.19, 125.56, 121.66, 121.40, 121.14, 114.57, 68.98, 68.70, 53.52.

1,3-Bis(5-phenyl-1H-1,2,3-triazol-1-yl) propan-2-ol (3i)
Green solid: mp. 233-236 °C, Lit[36] (mp. 233-236 °C). IR (KBr): ν= 688, 724, 763, 1074, 1125, 1278, 1464, 1729, 2860, 2928, 2959. ^{1}H NMR (400 MHz, DMSO) δ= 8.54 (s, 1H), 7.84 (m, 2H), 7.44-7.43 (m, 2H), 7.32-7.31 (m, 1H), 5.81 (m, 1H), 4.62-4.56 (d, 1H), 4.40 (m, 2H). ^{13}C NMR (100 MHz, DMSO) δ= 147.71, 132.42, 130.51, 129.68, 129.41, 127.11, 126.72, 124.12, 69.91, 54.84.

Results and discussion

Preparation and characterization of catalyst

Periodic mesoporous organosilicas (PMOs) represent an exciting new class of organic-inorganic nanocomposites targeted for application in catalysis. Organosilane precursor with a metal template imprinted ligand centre, an interphase catalyst is able to simulate homogeneous reaction condition, and at the same time it has the advantage of easy separation and recovery of the heterogeneous catalysts. In the present study, we use the interphase strategy to the preparation of a copper-imprinted periodic mesoporous organosilica nanocomposites (Cu@PMO NCs) for application as heterogeneous catalyst for three component synthesis of *β*-hydroxy-1,2,3-triazoles from epoxides, sodium azide and non-activated terminal alkynes. The first step in the accomplishment of this goal was the synthesis of (Cu@PMO NCs) (Scheme 1). To prepare the catalyst, initially ligand (**1**) was synthesized from the treatment of salicylaldehyde and melamine via a thermal method. Then, LCu (**2**) and copper-imprinted organopolysilane precursor (**3**) were prepared using $Cu(OAc)_2.H_2O$ and trimethoxysilyl moiety, respectively. Finally, the catalyst was obtained using a sol–gel process from a chemically synthesized organopolysilane precursor with a metal template (Cu^{2+} ion) imprinted ligand centre with tetraethylorthosilicate (TEOS) and cetyltrimethylammoniumbromide (CTAB) as a structural directing surfactant under basic conditions. The preparation procedure to obtain the catalyst (Cu@PMO NCs) is demonstrated in Scheme 1.

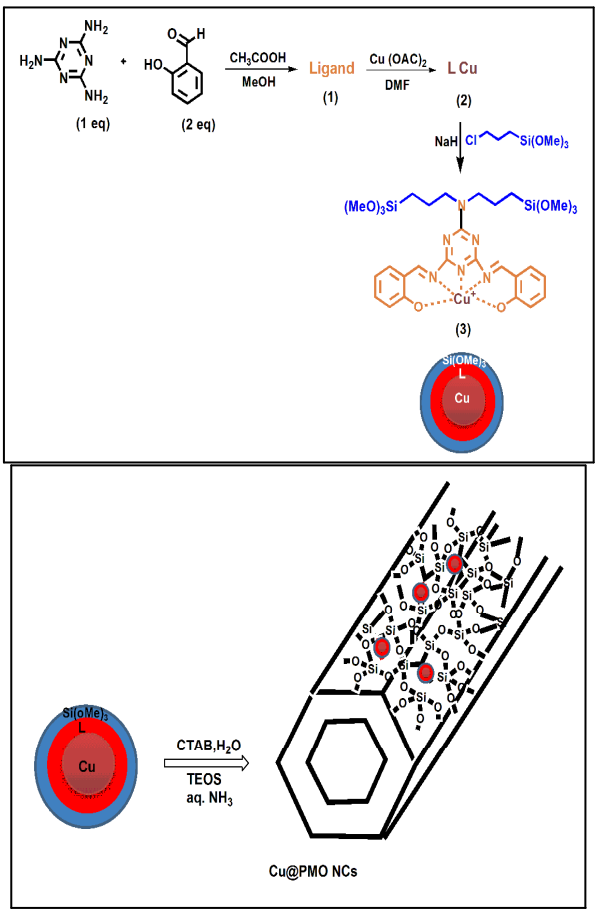

Scheme 1 General route for the synthesis of LCu (2), copper-imprinted organopolysilane precursor (3) and Cu@PMO NCs catalyst.

Characterization of catalyst

The X-ray diffraction (XRD) pattern of the Cu@PMO NCs was shown a sharp peak around 2θ= 0.9° and few weak peaks in 2θ=1.7-2.45°. The XRD spectram (Fig. 1) and FE-SEM image (Fig. 2-a) confirm the formation of the well-ordered two-dimensional (2D) hexagonal PMOs with a high content of copper template imprinted ligand centre groups. As can be clearly seen in Fig. 2, Cu@PMO NCs nanocomposite catalyst has spherical structure with size distribution approximately, 86 nm in size (Fig. 2-b).

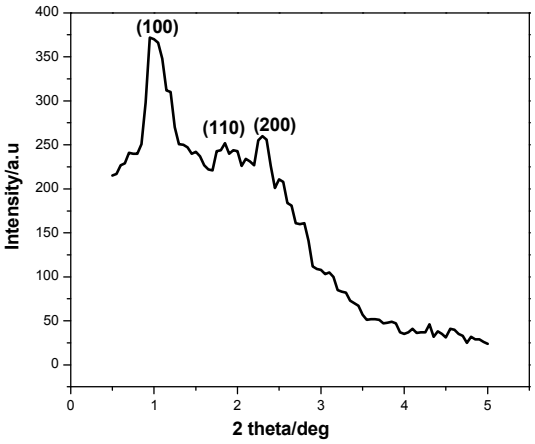

Fig. 1 XRD spectrum of Cu@PMO NCs

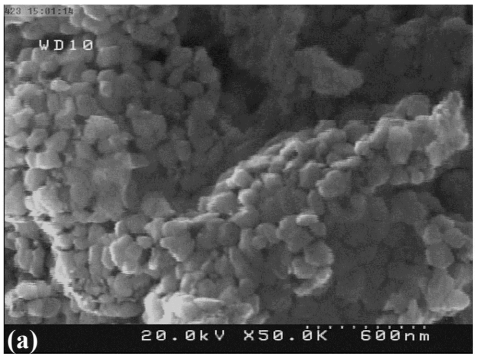

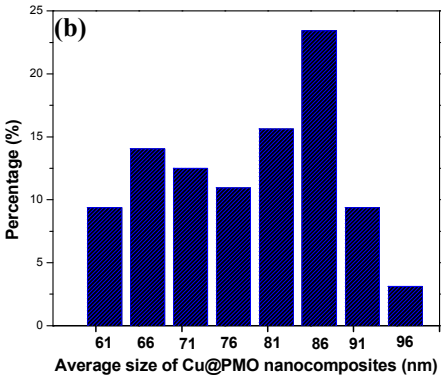

Fig. 2 (a) FE-SEM images of Cu@PMO NCs, (b) Distribution of Cu@PMO NCs framework by sizes according to FE-SEM data.

FT-IR confirms the presence of LCu (2) on PMO (Fig. 3). The C=N stretching vibration frequency of Cu@PMO NCs was observed at 1561 cm^{-1}. The vibration bands at 2853 and 2923 cm^{-1} were assigned to the C–H stretching vibrations of aromatic and aliphatic groups, respectively. The vibration peak at 1474 cm^{-1} was characteristic of N–C vibrations of the aromatic functional groups present in the Cu@PMO NCs. The band in the range 1000–1100 cm^{-1} was assigned to Si–O–Si groups and the band at 961 cm^{-1} was attributed to Si–OH groups. A broad band in the region, 3367 cm^{-1}, was assigned to the O–H stretching vibrations of surface silanols on Cu@PMO NCs.

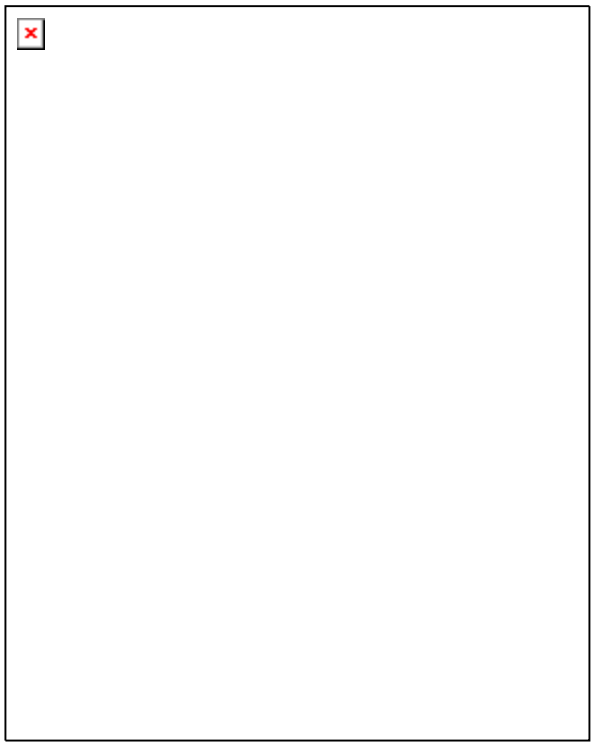

Fig. 3 FT-IR spectra of a) Ligand b) LCu and c) Cu@PMO NCs.

For Cu@PMO NCs, the results obtained by EDS were as follows (%): C, 18.42; N, 7.09; Cu, 3.43; Si, 24.73; O, 49.34 (Fig. 4). The EDS analysis is confirmed the presence of LCu on PMO. On the basis of the EDS, the amount of copper loading on Cu@PMO NCs was found to be 0.52 mmol Cu g^{-1}. In addition, AAS analysis indicates the presence of Cu in the catalyst and the content of Cu was estimated to be 0.47 mmol g^{-1}. The presence of copper on PMO framework was confirmed by two methods of analysis.

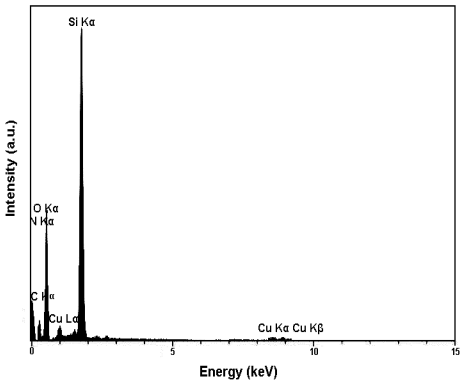

Fig. 4 EDS pattern of Cu@PMO NCs.

There is an evidence for oxidation state of Cu on the PMO which based on the UV–vis spectrum of LCu (**2**) and Cu@ PMO CPs as shown in Fig. 5. As clearly observed in this spectrum, the shift is observed in 267 to 348 nm in accordance to the formation of Cu (II)

during the addition of ligand. Comparison of UV-vis spectra for LCu (2) and Cu@ PMO CPs (diffuse reflective spectrum) confirms the presence of the anchored LCu(**2**) on the PMO (Fig. 5a). For further confidence about the oxidation state of copper in the complex form on the PMO framework the electrochemical properties of $Cu(OAc)_2.H_2O$ and Cu@ PMO CPs were investigated. In this experiment, the cyclic voltammograms of $Cu(OAc)_2.H_2O$ and Cu@ PMO CPs in 0.1 M KCl as supporting electrolyte was recorded with the scan rate of 100 mV s^{-1} using glassy carbon as working electrode (Fig. 5 b). One milligram of each complex was dispersed into water (100 µL) to provide a suspension. Next, 5 µL suspension was dropped on the cleaned GCE and allowed to dry at room temperature. Also, the cyclic voltammograms of 0.1 µM $Cu(OAc)_2.H_2O$ was carried out in supporting electrolyte. As can be seen from curve $Cu(OAc)_2.H_2O$, exhibits one peak (Ec= -0.37 V *vs.* Ag/AgCl) corresponding to the electron reductions of Cu (II) and formation of Cu (I) species. Also, in accordance to the curve Cu@ PMO CPs, the reduction of Cu(II) on the PMO was negatively shifted (Ec= -0.41 V *vs.* Ag/AgCl) comparing with those related to the $Cu(OAc)_2.H_2O$. Unexpectedly, these results reveals that $Cu(OAc)_2.H_2O$ and Cu@ PMO CPs shows partially cathodic shift.

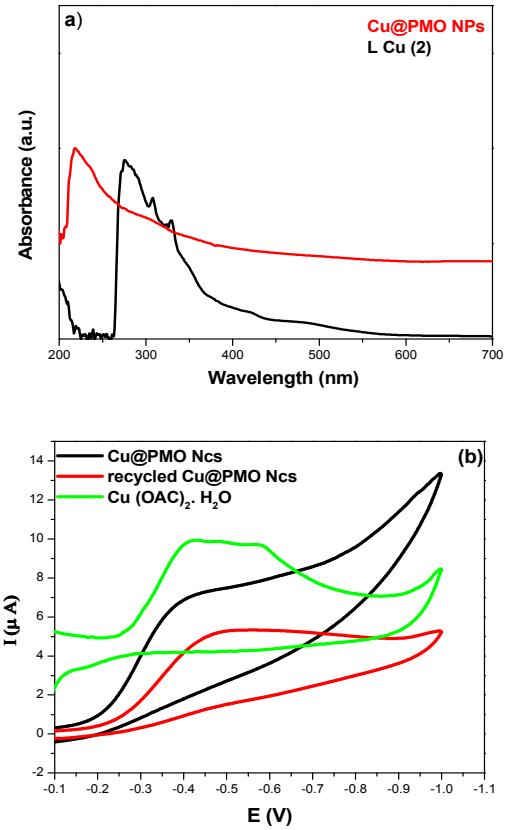

Fig. 5 (a) UV–vis spectra of Cu@PMO NCs and LCu (**2**). (b) Cyclic votammograms of Cu@PMO NCs, recycled Cu@PMO NCs. and $Cu(OAc)_2.H_2O$

However, several bonds are formed between the oxygen and nitrogens of ligand with Cu(II), that probably the main reason for the negative shift of complex comparing to that of $Cu(OAc)_2.H_2O$. Also, it seems that the oxidation state of Cu(II) remains after the reaction therefore, for this purpose, the cyclic voltammetry study of the recycled catalyst was done (Fig. 5). The cyclic voltammogram of recycled Cu@ PMO CPs was similar to Cu@ PMO CPs but shows that its reduction was negatively shifted (E=-0.49 V *vs.* Ag/AgCl) comparing with the votammogram related to the $Cu(OAc)_2.H_2O$.

A typical nitrogen adsorption/desorption type IV patterns with H3 hysteresis loops[37], which is characteristic of the highly ordered mesoporous materials, was obtained for Cu@PMO NCs. The BET specific surface area and a total pore volume were 462.40 $m^2 \cdot g^{-1}$ and 0.5 cm^3 g^{-1}, respectively (Fig. 6a). The pore diameter is calculated according to the BJH model to be 3.98 nm (Fig. 6b).

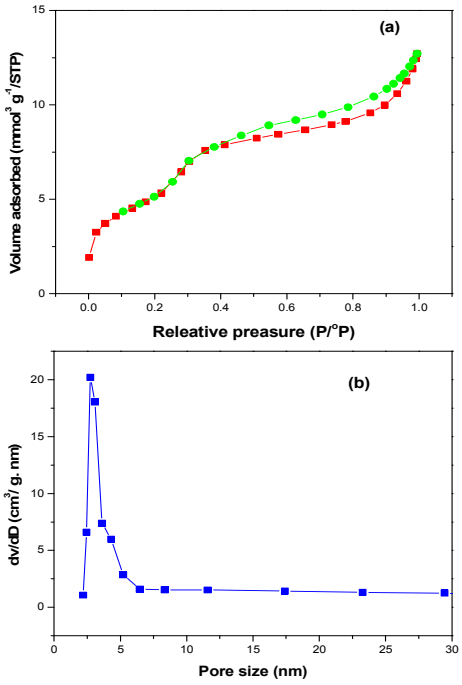

Fig. 6 N_2 adsorption-desorption isotherm (a) and pore size distribution curve (b) of Cu@PMO NCs.

TGA of Cu@PMO NCs shows two major weight losses at 25-800 ºC in a nitrogen atmosphere (Fig. 7). A weight loss of less than 3 % between 100-250 ºC is observed, probably due to physical absorbed water. The sharp weight loss from 300 to 800 ºC results from the decomposition of LCu (**2**)-bridging groups, suggesting a stable organic–inorganic composite framework (22 %). In addition, TGA analysis indicated that the prepared Cu@PMO NCs catalyst has high thermal stability and negligible LCu (**2**) leaching up to about 300 °C. Based on TGA analysis, the amount of loaded LCu (**2**) on the Cu@PMO NCs nanocomposites catalyst was 52.62 mmol LCu (**2**) g^{-1}.

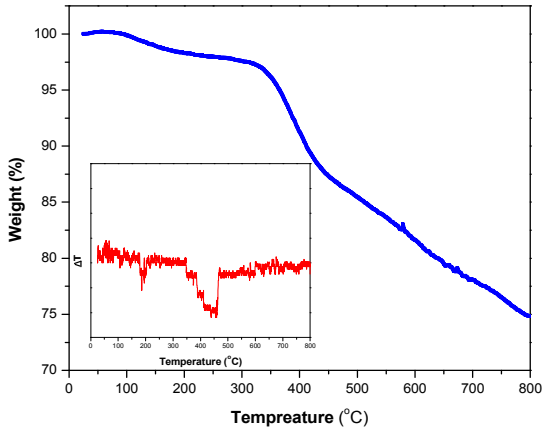

Fig. 7 TGA-DTA thermograms of Cu@PMO NCs catalyst.

Experimental design in the *β*-hydroxy-1,2,3-triazole (3a)

To find out the optimization conditions for the reaction, a series of experiments were performed with the standard reaction of styrene oxide, phenylacetylene and sodium azid as a model reaction (Scheme. 2). In order to evaluate the effect of ultrasound irradiation on *β*-hydroxy-1,2,3-triazole (**3a**) production using the Cu@PMO NCs as catalyst, the effect of different variables such as ultrasound irradiation frequency, Cu@PMO NCs amount (%) and ultrasound time (min) in the three component reaction were investigated. The influence of these variables was observed through an experimental design [Box-Behnken design (BBD)] using the surface response.

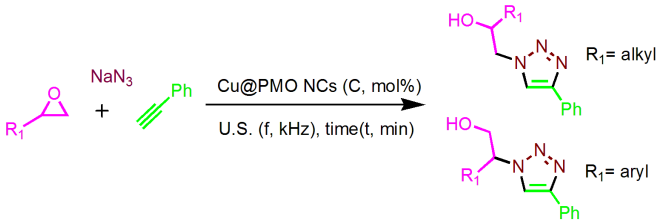

Scheme 2 Three-component synthesis of *β*-hydroxy-1,2,3-triazoles.

Effects of major variables

The effect of variables which were significant in the process could be evaluated based on the values of (p) (Table 2). As shown in Table 2, the amount of Cu@PMO NCs had a positive effect on *β*-hydroxy-1,2,3-triazole (3a) yield (6.00). Variable of ultrasound irradition frequency was shown low effect (0.375) on reaction catalyzed by Cu@PMO NCs. Another important variable to consider was done the duration of the reaction. This also had a low effect (0.125) on the reaction.

Table 2 Effect of the parameters estimates for the *β*-hydroxy-1,2,3-triazole **(3a)** production.

Variables	Effect	Standard error	*p*-Value
Mean	98.000	1.103	<0.0001
Cu@PMO NCs content (C)	6.000	0.675	<0.0001
Ultrasound irradiation frequency (F)	0.375	0.675	0.603
Ultrasound time (t)	0.125	0.675	0.860
C × C	-6.37	0.994	0.001
F × F	-5.12	0.994	0.004
t × t	-4.12	0.994	0.009
C × F	-1.500	0.955	0.177
C × t	-0.000	0.955	1.000
F × t	-4.250	0.955	0.007

The effect of variables on the *β*-hydroxy-1,2,3-triazole (**3a**) production under ultrasound irradiation catalyzed by Cu@PMO NCs can be clearly observed in the surface response graphs that is shown in Fig. 8. Fig. 8a described the variation of yield of *β*-hydroxy-1,2,3-triazole (3a) regarding the amount of catalyst and ultrasound irradiation frequency.The yield increased rapidly to an optimum value with the increase of catalyst amount and thereafter declined slightly as the microwave power increased. It is apparent that the amount of catalyst played a more vital part in the reaction than ultrasound irradiation frequency, and the interaction between these two variables was significant. Fig. 8b illustrated the correlation of amount of catalyst and ultrasound time. As the ultrasound time extended, the response improved dramatically to the highest value and thereafter dropped. The decrease might be due to the degradation of *β*-hydroxy-1,2,3-triazole (3a) in the later reaction stage. On the basis of response surface, the yield of *β*-hydroxy-1,2,3-triazole (3a) was more sensitive to the amount of catalyst than to ultrasound time. Yield of *β*-hydroxy-1,2,3-triazole (3a) as a function of ultrasound irradiation frequency and ultrasound time, was presented in Fig. 8c. According to the features of the graph and results reported in the Table 2, indicated that ultrasound irradiation frequency was a more crucial factor for reaction than ultrasound time.

Based on the quadratic model, the optimum yield of *β*-hydroxy-1,2,3-triazole (3a) catalyzed by Cu@PMO NCs under ultrasound irradition frequency was predicted to be 99 % under the conditions as follows: amount of catalyst 0.007 g (0.33 mol %), ultrasound irradition frequency of 40 kHz and ultrasound time of 7 min (Table 1, entry 1).

The quadratic model which predicted the relationship between yield of *β*-hydroxy-1,2,3-triazole (3a) (y) with independent variables was expressed by Eq. (1):

$$y= 89.00 +6.00C +0.37 F +0.12 t -6.37 C^2 -5.12 F^2-4.12 t^2-1.50 C \times F -4.25 F \times t \quad (1)$$

Where y is the percentage of yield conversion and, C, F and t are coded values of Cu@PMO NCs content, irradiation frequency and ultrasound time, respectively

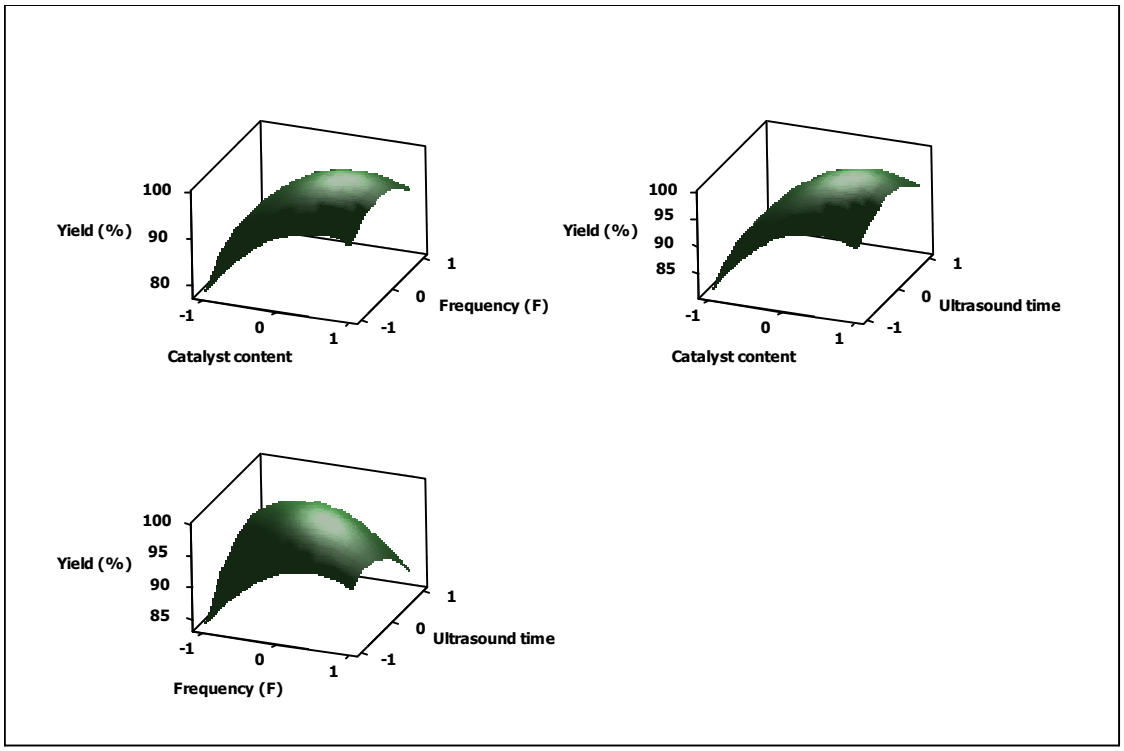

Fig. 8 Fitted response surface for the reaction

Heterogeneity test

Any leaching of the active species from the support makes the catalyst unattractive, and hence, it is necessary to study the stability as well as leaching of LCu (**2**) from the support. For the rigorous proof of heterogeneity, a test was carried out by filtering the catalyst from the reaction mixture under ultrasound irradiation after 3.5 min and the filtrate was allowed to react up to 15 min. After the 3.5 min, the solid product and catalyst was separated from the reaction mixture by dissolving in hot methanol (see experimental section) to give the corresponding product **3a** in 47 % yield. After up to 15 min, it was no observed solid product from the reaction mixture. It was found from the heterogeneity test that there was not solid product up to 15 min. On the basis of these results, it can be concluded that there is no leaching of LCu (**2**) species from the support PMO.

Also, the leaching of Cu from Cu@PMO NCs was confirmed by carrying out the analysis of AAS from the filtrated solution and there is no deactivation of catalyst. Hence, this analysis strongly suggests no leaching of any active species, Cu@PMO NCs, and the present catalyst is truly heterogeneous in nature.

Recycling of the catalyst

One of the main aims of this work was to develop the ease of recovery and recycling of the heterogeneous catalyst. We further explored the reusability of the catalyst in the model reaction with treatment of the styrene oxide, the phenylacetylene, NaN_3 in the presence of 0.33 mol % of Cu@PMO NCs catalyst under ultrasound irradiation (40 kHz) in H_2O at room temperature for 7 min. The catalyst was easily and completely separated from the reaction mixture by simple filtration, washed with double distilled water and dried at 100 ºC in an oven for 3 h, and the recovered catalyst was

charged for the further run. The corresponding results indicated that this simple separation method could be repeated for 6 consecutive runs and the recovered catalyst showed remarkably constant catalytic activity in all the 6 cycles (Fig. 9).

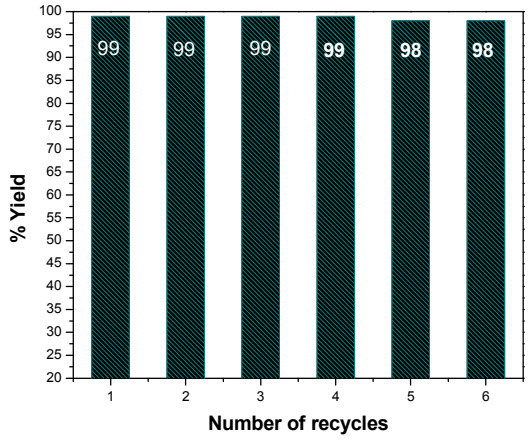

Fig. 9 Recycling of the Cu@PMO NCs catalyst.

Comparison with the reported catalysts

We took on a comparative study on the reactivity of the Cu@PMO NCs with a variety of copper catalysts under standard condition of 1,3-dipolar cycloaddition of styrene oxide, sodium azide, and phenylacetylene. This fact is observed from Table 3 that much higher yields were obtained for *β*-hydroxy-1,2,3-triazoles using this catalyst, also the amount of required catalyst is low copper loading (0.33 mol %, 0.007 g) in comparison with the other reported catalysts (Table 3, entries 2, 3) and the commercial copper (Table 3, entry 1).

Table 3 Three components synthesis of *β*-hydroxy-triazoles catalyzed by copper on different supports

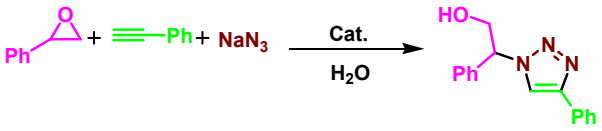

Entry	Catalyst	Catalyst amount (mol %)	t (°C)	T (h)	Yield (%)
1	$Cu(OAc)_2.H_2O$	10	70	24	0
2	Cu^I-Zeolite [a]	8	25	20	77
3	Cu@ phosphorated SiO_2	0.64	60	1	94
4	Cu@PMO NCs [b]	0.33	25	0.12	99

[a] Zeolite loading of 20 mg (ca. 0.08 mmol Cu(I)).
[b] Ultrasound irradiation (40 kHz), ultrasound time, 7 min.

High efficiency and generality of synthesis of *β*-hydroxy-1,2,3-triazoles under optimized conditions

After detecting more efficient catalyst amount (0.33 mol %), ultrasound time (7 min) and ultrasound irradition frequency (40 kHz) to delineate the role of ultrasound, this methodology have also developed an experimentally convenient one-pot, regioselective synthesis of *β*-hydroxy-1,2,3-triazoles from epoxides, sodium azide, and phenylacetylene in water at room temperature. Ultrasonic-assisted chemistry was used due to the efficiency of the interaction of ultrasound irradiation with the nanocatalyst. When the reaction was carried out under optimized condition (frequency (40 kH), Cu@PMO NCs (0.33 mol %) and ultrasound time (7 min)), it gave excellent yields of product in short ultrasound time. The results are summarized in Table 4. The substitution of aryl on the epoxides, the yield of reaction was found to be relatively high and the reaction was completed within 7 min (Table 4, entries 1,2). The reaction of alkyl epoxides in this procedure were shown relatively lower yields (Table 4, entries 3–10), also cyclooctene oxide (1f) and cyclododecene oxide (1g) did not reacted and remained unchanged even after extended ultrasound irradiation and ultrasound time until 8 h (Table 4, entries 11, 12). Furthermore, the results show that Cu@PMO NCs is a highly efficient catalytic system for the cycloaddition of alkyl and aryl epoxides with phenylacetylene.

The proposed mechanism for the formation of *β*-hydroxy-1,2,3-triazoles includes 2 pathways in which Cu@PMO NCs has a twofold catalytic role as a bifunctional catalyst, which combines two reactions as one-pot ring opening and 1,3-dipolar cycloaddition. Firstly, the participation of a metal azide as the catalytically active species suggests that the mechanism of epoxide ring opening involves azide delivery from the catalyst as well as epoxide activation by the Cu@PMO NCs catalyst and formation of organoazide. On the other hand, the π-complex formation between the phenylacetylene and Cu@PMO NCs to afford the copper (II) acetylide, follows the 1,3-dipolar cycloaddition between the copper(II) acetylide and organoazide, than final protonolysis of the resulted intermediate would render the *β*-hydroxy-1,2,3-triazole product. Moreover, according to the above description related to the cyclic voltametric studies on Cu@PMO NCs catalyst (Fig. 5 b) before and after the reaction was confirmed the oxidation state of (2+) for Cu. However, the different works were reported that the copper (II) as a catalyst without any reducing agent played the catalytic rule in the click reaction[16, 38].

Table 4 Three component synthesis of *β*-hydroxy-1,2,3-triazoles from epoxides 1a-m, phenylacetylene, sodium azide catalyzed by Cu@PMO NCs in water[a]

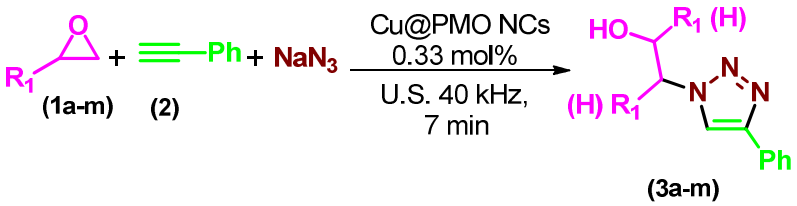

Entry	Epoxide	Triazol	Yield[b] (%)	TON[c]/TOF[d]
1	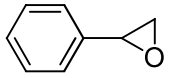 (1a)	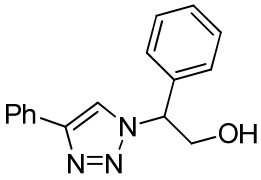 (3a)	99	341.37/48.76
2	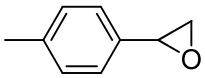 (1b)	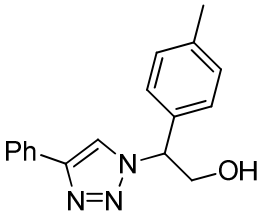 (3b)	99	341/48.76
3	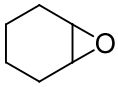 (1c)	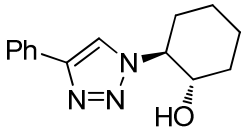 (3c)	86	296.55/42.36
4	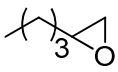 (1d)	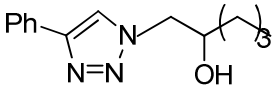 (3d)	80	275.86/39.40
5	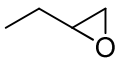 (1e)	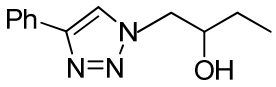 (3e)	86	296.55/42.36
6	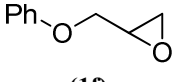 (1f)	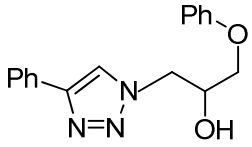 (3f)	89	306.89/43.84

7	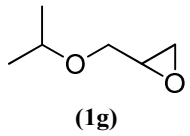 (1g)	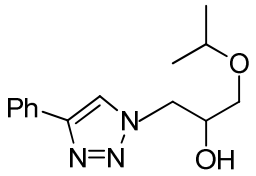 (3g)	79	272.41/38.91
8	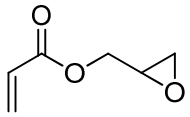 (1h)	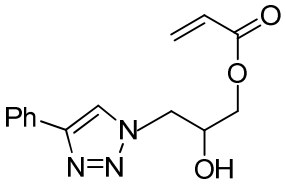 (3h)	76	262.06/37.43
9	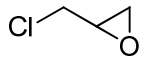 (1i)	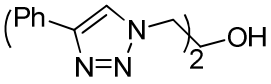 (3i)	74	255.17/36.45
10	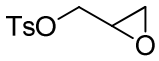 (1j)	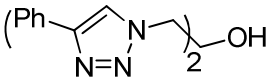 (3i)	78	268.95/38.42
11[e]	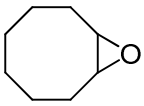 (1k)	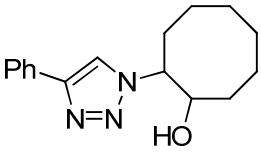 (3k)	-	-
12	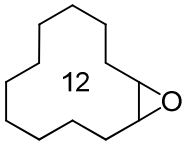 (1l)	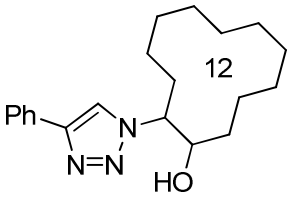 (3l)	-	-

[a] Reaction condition: epoxide (1 mmol), Phenylacetylene (1 mmol), NaN_3 (1.1 mmol), Cu@PMO NCs (0.007 g, 0.33 mol % Cu), H_2O, under ultrasound irradiation (40 kHz), at room temperature, ultrasound time, 7 min.
[b] Isolated yields.
[c] TON: Mole of formed *β*-hydroxy-1,2,3-triazole per mole of catalyst.
[d] TOF: TON per time (min).
[e] The reaction was done with 1:2:2 mol ratio of epoxide, alkyne and NaN_3 respectively

Conclusions

This research project therefore mainly consists of two parts, one is the synthesis, characterization and the testing on the catalyst activity of Cu@PMO NCs, and another part is the Box-Behnken design which was used to design an experimental program to provide data to model the effects of catalyst amount , ultrasound irradiation frequency and ultrasound time on *β*-hydroxy-1,2,3-triazole yields. The preparation and characterization of copper catalyst based on ligand functionalized PMO were described. The resulting copper-imprinted periodic mesoporous organosilica nanocomposite (Cu@PMO NCs) perform as highly efficient and reusable

catalyst for the synthesis of β-hydroxy-1,2,3-triazoles. The mathematical model proposes a satisfactory representation of the process and a good correlation between theoretical values provided by the model equation and experimental results. Thus, Box-Behnken design was implemented as a tool to evaluate the optimized reaction conditions, and it is way of obtaining the maximum amount of yield with the fewest number of experiments and saving time. It was developed a quick and highly efficient method for copper-catalyzed cycloaddition of water insolution aryl/alkyl epoxides and alkynes at room temperature. Altogether, the simplicity in operation, use of water solvent, reaction at ambient temperature under ultrasound irradiation, excellent yields, no need for chromatographic purification, shorter reaction time, high capacity and recyclability of the catalyst, makes this procedure a valid candidate towards the goal of green chemistry.

References

1. V. Rebbin, R. Schmidt and M. Fröba, *Angew. Chem. Int. Ed.*, 2006, **45**, 5210–5214.
2. C. V. Polshettiwar, C. Len and A. Fihri, *Chem. Rev*, 2009, **253**, 2599.
3. H. H. Yang, S. Q. Zhang, W. Yang, X. L. Chen, Z. X. Zhuang, J. G. Xu and R. X. Wang, *J. Am. Chem. Soc.*, 2004, **126**, 4054–4055.
4. G.-Z. Fang, J. Tan and X.-P. Yan, *Anal. Chem.*, 2005, **77**, 1734–1739.
5. Y.-K. Lu and X.-P. Yan, *Anal. Chem.*, 2004, **76**, 453–457.
6. M. C. Bruzzoniti, A. Prelle, C. Sarzanini, B. Onida, S. Fiorilli and E. Garrone, *J. Sep. Sci.*, 2007, **30**, 2414–2420.
7. R. Ouyang, J. Lei and H. Ju, *Chem. Commun.*, 2008, **44**, 5761–5763.
8. K. Haupt, *Anal. Chem.*, 2003, **75**, 376–383.
9. G. Wuff, *Chem. Rev.*, 2002, **102**, 1–27.
10. F. L. D. A. Mujahid and P.A. Lieberzeit, *Materials*, 2010, **3**, 2196–2217.
11. M. S. Moorthy, P. K. Tapaswi, S. S. Park, A. Mathew, H. Cho and C. Ha, *Micropor. Mesopor. Mater.*, 2013, **180**, 162–171.
12. R. Huisgen, *Pure Appl. Chem*, 1989, **61**, 613–628.
13. R. Huisgen, G. Szeimies and L. Moebius, *Chem. Ber.*, 1965, **98**, 4014–4021.
14. V. V. Rostovtsev, L. G. Green, V. V. Fokin and K. B. Sharpless, *Angew. Chem., Int. Ed.*, 2002, **41**, 2596–2599.
15. K. R. Reddy, C. U. Maheswari, M. L. Kantam and P. C. Division, *Synth. Commun*., 2008, **38**, 2158–2167.
16. N. Mukherjee, A. Sabir, S. Bhadra and B. C. Ranu, *Green.Chem*, 2013, **15**, 389–397.
17. F. Wang, H. Fu, Y. Jiang and Y. Zhao, *Green Chem*, 2008, **10**, 452.
18. L. S. Campbell-Verduyn, W. Szymański, C. P. Postema, R. A. Dierckx, P. H. Elsinga, D. B. Janssen and B. L. Feringa, *Chem. Commun.*, 2010, **46**, 898–900.
19. R. B. Nasir Baig and R. S. Varma, *Green Chem*, 2012, **14**, 625.
20. P. Appukkuttan, W. Dehaen, V. V Fokin and E. Van Der Eycken, *Org. Lett*, 2004, **6**, 4223–4225.
21. J. García-Álvarez, J. Díez and J. Gimeno, *Green Chem*, 2010, **12**, 2127.
22. T. Miao and L. Wang, *Synthesis*, 2008, **3**, 363–368.
23. F. Alonso, Y. Moglie, G. Radivoy and M. Yus, *J. Org. Chem.*, 2011, **76**, 8394–405.
24. F. Alonso, Y. Moglie, G. Radivoy and M. Yus, *Adv. Synth. Catal.*, 2010, **352**, 3208–3214.
25. T. Boningari, A. Olmos, B. M. Reddy, J. Sommer and P. Pale, *Eur. J. Org. Chem*, 2010, **33**, 6338–6347.
26. H. Naeimi and V. Nejadshafiee, *New J. Chem.*, 2014, **38**, 5429–5435.
27. H. Sharghi, M. H. Beyzavi, A. Safavi, M. M. Doroodmand and R. Khalifeh, *Adv. Synth. Catal*., 2009, **351**, 2391–2410.
28. H. Sarvari, M. Moeini, F. Khalifeh, R. Beni and A. Salimi, *Helv. Chim. Acta.*, 2010, **93**, 435–449.
29. M. Ashokkumar and T. J. Mason, *Encyclopedia of Chemical Technology*, 2007.
30. J. K. Kim, F. Martinez and I. S. Metcalfe, *Catalysis Today*, 2007, **124**, 224–231.
31. M. Driowya, A. Puissant, G. Robert, P. Auberger, R. Benhida and K. Bougrin, *Ultrason. Sonochem.*, 2012, **19**, 1132–1138.
32. B. A. Dar, A. Bhowmik, A. Sharma, P. R. Sharma, A. Lazar, A. P. Singh, M. Sharma and B. Singh, *Appl. Clay Sci.*, 2013, **81**, 351–357.
33. K. M. Goncalves, F. K. Sutili, S. G. F. Leite, R. O. M. A. Souza and R. C. I. Leal, *Ultrason. Sonochem.*, 2012, **19**, 232–236.
34. A. Tsirk, S. G. I and A. Hiirnfeldt, *Tetrahedron*, 1998, **54**, 1817–1834.
35. J. S. Yadav, B. V. S. Reddy, G. M. Reddy and D. N. Chary, *Tetrahedron Lett.*, 2007, **48**, 8773–8776.
36. T. Boningari, A. Olmos, B. M. Reddy, J. Sommer and P. Pale, *Eur. J. Org. Chem*., 2010, **33**, 6338–6347.

37. G. Leofanti, M. Padovan, G. Tozzola and B. Venturelli, *Catalysis Today*, 1998, **41**, 207–219.

38. K. Namitharan, M. Kumarraja, and K. Pitchumani, *Chem. Eur. J.,* 2009, **15**, 2755–2758.